Diffuse Radio Emission in Galaxy Clusters Insights With Primary Electron Model

BY

Yadessa Chewaka Aga

A PROJECT SUBMITTED TO

GRADUATE PROGRAMS OF
ADDIS ABABA UNIVERSITY

IN PARTIAL FULFILLMENT FOR THE REQUIREMENTS
OF THE DEGREE

MASTER OF SCIENCE IN PHYSICS

ASTROPHYSICS

ADDIS ABABA, ETHIOPIA

SEPTEMBER, 2024

ADDIS ABABA UNIVERSITY

COLLEGE OF NATURAL AND COMPUTATIONAL SCIENCES

DEPARTMENT OF PHYSICS

PROGRAM OF GRADUATE STUDIES

Diffuse Radio Emission in Galaxy Clusters

Insights With Primary Electron Model

By

Yadessa Chewaka Aga

Approved by the Examining Board:

Member	**Signature**
Advisor	_____
First Examiner	_____
Second Examiner	_____

Date: September, 2024

ADDIS ABABA UNIVERSITY

Date: **September 2024**

Author:

Title:

Department: **Department of Physics**

Degree: **M.Sc.** Convocation: **September** Year: **2024**

Permission is herewith granted to Addis Ababa University to circulate and to have copied for non-commercial purposes, at its discretion, the above title upon the request of individuals or institutions.

_____

Signature of Author

This Work is Dedicated

to

Konjit Regassa Negewo

Table of Contents

List of Tables

List of Figures

Acknowledgements

I would like to express my deepest gratitude to the Almighty God, who has guided me throughout my life's journey and in all my endeavors.

My heartfelt appreciation goes to my advisor, Dr.Negessa Tilahun, for his constructive criticism, insightful comments, and continuous support, which have been invaluable to the success of this research.

I am also profoundly grateful to my brother, Samuel Belete, whose encouragement and unwavering support have propelled me forward in my educational pursuits. His guidance has made this journey meaningful.

I also express my heartfelt love and respect to my friend Hashim Jemal Essa who has always encouraged me by sharing his experience and knowledge with me day and night.

Lastly, I extend my deepest thanks to my wife, Konjit Regassa, for providing the necessary resources and a conducive environment that contributed significantly to the success of this work. Without her support, this work would not have been completed.

Addis Ababa University

Yadessa Chewaka Aga

Abbreviations

AGN	Active Galactic Neclues
DSA	Diffusive Shock Aceleration
GMRT	Gaint Metric Radio Telesscope
ICM	Intercluster Medium
MHD	Magnotohydrodynamic
VLA	Very Large Array
WENSS	The Westerbork Northern Sky Survey
WSRT	Westerbork synthesis Radio Telescope
SETI	Search for Extraterrestrial Intelligence
SKA	Square Kilometre Array
LOFAR	Low Frequency Array
CMB	Cosmic Microwave Background
AME	Anomalous microwave emission
XRISM	X-ray Imaging and Spectroscopy Mission

Physical Constants

Mass of the Sun	$M_\odot$ = 1.99 $\times$ 10^{33} g
Kilo parsec	kpc = 3.08568025$\times 10^{21}$ cm
Speed of Light	C = 2.99792458$\times$ 10^{8} ms^{-2}
Universal Gravitational Constant	G = 6.67$\times 10^{-11} Nm^2 kg^{-2}$
Mega parsec	Mpc = 3.08568025$\times 10^{24}$ cm
Luminosity of the Sun	$L_\odot$ = 3.839 $\times 10^{33}$erg/s
Hobble's constant	H_0 = 70.65km/s/Mpc

Symbols

L	Total radiated luminosity in erg/s
D_l	Luminosity distance of the from the source to Earth in Mpc
S_{GW}	Power spectral density in unit of egr/sHz
z	Redshift
α	Spectral Index
$P_{1.4}$	Radio Power
L_x	X-ray Luminosity
LLS	Linear size of the radio emission
γ	Lorentz factor

Abstract

Diffuse extended radio sources are found as the number of galaxy clusters increases. The radio emission reveals the presence of cosmic rays and magnetic fields in the ICM. The relativistic electrons undergo diffuse radio emission and lose their energy via inverse-Compton and synchrotron losses in a short time, typically having lifetimes of about 0.1 Gyr. They could last for Gyr if significant re-acceleration is involved. Diffuse cluster radio sources are classified into radio halos, cluster radio shocks (relics), and revived AGN fossil plasma sources. This study summarizes the properties of diffuse cluster radio sources, providing significant insights and provides key insights into the complex interplay between relativistic electrons and the surrounding environment, enhancing our learning of cosmic structure formation.

CHAPTER 1

Introduction

1.1 Back Ground to Radio Wave in Galaxy Clusters

Galaxy clusters are among the largest gravitationally bound structures in the universe, containing vast amounts of dark matter, hot gas, and galaxies. One notable feature of many galaxy clusters is the presence of diffuse radio emission, which manifests as large-scale, low-surface-brightness structures. This emission is primarily attributed to synchrotron radiation produced by relativistic electrons spiraling around magnetic fields.

In this study, we focus on the primary electron model, which posits that the diffuse radio emission results from high-energy electrons accelerated by various processes within the cluster. These processes may include shock waves from merging clusters, turbulence in the intracluster medium, and interactions between cosmic rays and thermal particles. By employing this model, we aim to deepen our understanding of the origins and characteristics of radio emission in galaxy clusters, as well as its implications for the physics of cosmic ray propagation and magnetic field dynamics.

We will analyze observational data from recent radio surveys, alongside theoretical predictions and simulations, to explore how the primary electron model can account for the observed properties of diffuse radio sources. Our investigation seeks to bridge the gap between observational astrophysics and theoretical models, providing a comprehensive view of the mechanisms driving diffuse radio emission in galaxy clusters.

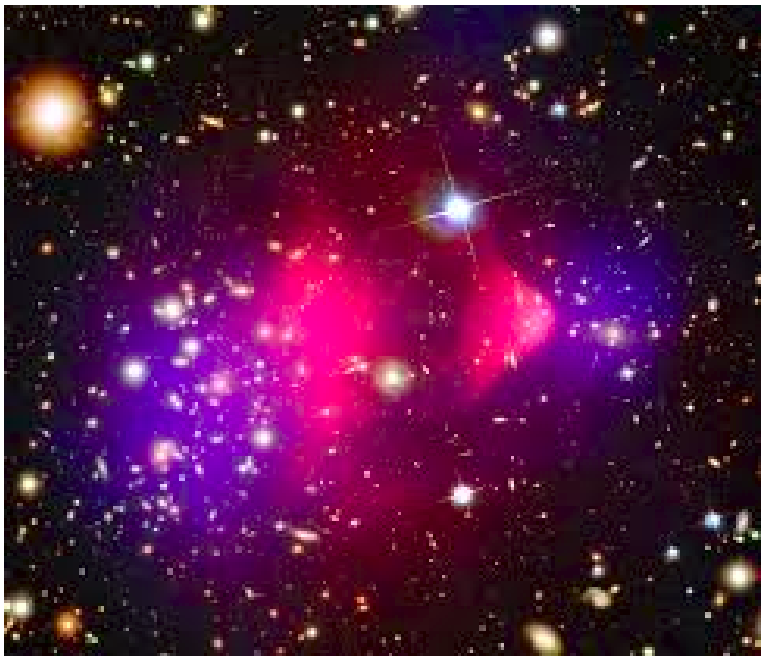

Figure 1.1: Diffuse Radio sources [3]

In this chapter, a clear theoretical background to emissions of particles, life time of radiating electrons, the energy loss, acceleration mechanisms of cosmic ray electrons, which are vital in radio halo generation in clusters with magnetic field strength of a few μG discussed, and halo spectra observations [8]. The main process at the origin of the radio emission in the universe is the synchrotron process. Its spectral and polarization properties give important information on the physics and evolution of the radio sources. Radio emissions from AGNs and the ICM are caused by synchrotron radiation. The radiation is produced by the spiraling motion of relativistic electrons in a magnetic field. The power emitted by a relativistic electron depends on its energy γ and on the magnetic field strength. The higher field strength, the lower the electron energy is needed to produce emission at a given frequency [8].

1.1.1 History of Radio Astronomy

- **Early 20th Century:** The foundation of radio astronomy began with the discovery of radio waves by Heinrich Hertz in the 1880s, demonstrating that electromagnetic waves could be generated and detected.

- **1930s:** Karl Jansky, a Bell Telephone Laboratories engineer, is often credited as the first radio astronomer. In 1931, he detected radio waves from the Milky Way while investigating sources of static interference for transatlantic radio communications.
- **1940s:** Following World War II, interest in radio technology surged. Researchers like Grote Reber built the first dedicated radio telescope in 1937, conducting systematic observations of celestial radio sources.
- **1950s:** The field expanded rapidly with the advent of larger telescopes and the discovery of various astronomical phenomena, including quasars and pulsars. The first pulsar was discovered by Jocelyn Bell Burnell and Antony Hewish in 1967.
- **1960s-1970s:** Advancements in technology led to the development of more sophisticated radio telescopes and arrays, including the VLA in New Mexico.
- **1980s-Present:** Radio astronomy has grown into a crucial branch of astrophysics, enabling the study of the cosmic microwave background radiation, the structure of galaxies, and the SETI.

Today, radio astronomy plays a vital role in our understanding of the universe, allowing scientists to explore phenomena that are invisible in optical wavelengths.

1.2 A History of the Observation of Diffuse Radio Emission in Galaxy Clusters

The observation of diffuse radio emission in galaxy clusters has evolved significantly over the past several decades, reflecting advancements in both observational techniques and theoretical understanding in astrophysics. The study of radio emissions from galaxy clusters began in the mid-20th century (1950s-1970s). Initial hints of diffuse radio emission emerged in the 1970s with the identification of extended sources in cluster environments. Notably, the discovery of the Coma Cluster

as a source of diffuse radio emission marked a pivotal moment [1].

In the 1980s and 1990s, researchers developed theoretical models, such as the primary electron model, to explain the diffuse radio emissions observed in clusters. The advent of new radio telescopes like LOFAR and GMRT in the 2000s revolutionized the study of galaxy clusters with advanced observational techniques. The 2010s saw a shift toward multi-wavelength studies, enabling researchers to correlate diffuse radio emissions with the thermal properties of the ICM.

Ongoing advancements, including the development of next-generation telescopes like the SKA, promise to provide deeper insights into the complex interactions within clusters. Diffuse cluster radio sources are categorized into three main classes: halos, mini-halos, and relics [9]. Mini-halos are smaller and found in relaxed cool-core clusters, while radio relics are extended sources with high polarization at GHz frequencies, located in the cluster periphery.

This paper focuses particularly on halos. A radio filament is also proposed, hinting at large-scale filaments of the cosmic web outside of clusters. Current models and observations are mainly restricted to high-mass, low-redshift clusters, but there is potential for discovering diffuse emissions in lower mass and higher redshift systems. Evidence collected is summarized in Table 1, and ongoing observational campaigns aim to enhance the understanding of radio halos and relics in galaxy clusters.

The study holds several important implications for both astrophysics and cosmology. By investigating diffuse radio emissions, it provides insights into complex processes occurring in galaxy clusters, including interactions between galaxies, dark matter, and the intergalactic medium. This research enhances understanding of the origins and behavior of cosmic rays, particularly primary electrons, which are key to high-energy phenomena. The findings will help correlate radio emissions with X-ray observations, providing a multi-wavelength perspective that enriches our understanding of cluster physics. Insights gained could influence current models of cosmic evolution and structure formation. The methodologies developed may

enhance observational techniques and data analysis methods in radio astronomy, benefiting future research.

Overall, this study is significant not only for its scientific contributions but also for its potential to influence broader discussions in cosmology and our understanding of the universe's fundamental processes.

1.3 Focus of the Study

The focus of the study titled "Diffuse Radio Emission in Galaxy Clusters: Insights from the Primary Electron Model" is to investigate the mechanisms and characteristics of diffuse radio emissions in galaxy clusters, specifically through the lens of the primary electron model.

1.3.1 Diffuse Radio Emission

This area involves understanding the nature and origin of radio emissions observed in galaxy clusters and exploring how these emissions are linked to the presence of high-energy electrons.

1.3.2 Primary Electron Model

This section examines the role of high-energy electrons in producing synchrotron radiation and identifies the acceleration processes that contribute to the generation of these electrons, including shock waves from merging clusters, turbulence in the ICM, and cosmic ray interactions with thermal particles. Generally, the study aims to enhance understanding of the physical processes occurring in galaxy clusters and their relation to the broader cosmic environment.

1.4 Objectives

1.4.1 General Objective

The general objective of the study is to investigate diffuse radio emission in galaxy clusters through insights from the primary electron model.

1.4.2 Specific Objectives

Specific objectives include:

- To determine the origins of diffuse radio emission in galaxy clusters.
- To identify mechanisms that accelerate primary electrons within galaxy clusters, including shock waves from mergers and AGNs.
- To explore the implications of diffuse radio emission, particularly the contribution of primary electrons.

1.5 Methodology

The study utilizes a combination of observational and analytical methods, preferring theoretical frameworks and integration techniques. To analyze synchrotron radiation emitted by primary electrons, a structured theoretical methodology is applied, providing a framework for understanding the underlying physics and modeling the radiation properties. By employing various techniques, researchers can gain deeper insights into particle acceleration mechanisms, magnetic field configurations, and the dynamics of astrophysical phenomena [9].

The integration of observed spectra with theoretical models will enhance understanding of the acceleration mechanisms of primary electrons. These methods collectively enable a thorough investigation of diffuse radio emissions in galaxy clusters, providing valuable insights into the underlying astrophysical processes.

The organization of this thesis is; in Sect.2 Reacceleration Mechanisms. In Sect.3 Observation of Diffuse Radio Emission in galaxy. In Sect.4, Primary electron Model and in sect.5 Summary.

CHAPTER 2

Radio Emission Mechanisms

2.1 Reacceleration Mechanisms

Over the past century, a great deal of observational evidence has been recorded for the presence of highly relativistic particles in some astrophysical objects. In this chapter, we will review the mechanisms, evidence, and implications. As in dark matter searches, the evidence for fast particles in astrophysical sources may be divided into direct and indirect evidence. Direct evidence consists of observations of actual relativistic particles, i.e., cosmic rays, while indirect evidence comprises observations of secondary products of fast particles, i.e., everything else. Observati-ons of high-energy photons and neutrinos count as indirect evidence, because electr-ically neutral particles cannot be accelerated directly; they must be produced secon-darily, as a result of either collisions between particles or interactions between particles and magnetic fields. Direct and indirect detection are regarded as comple-mentary in dark matter searc-hes because they have different sensitivities and sources of systematic error. Howe-ver, in principle, either direct or indirect detection could suffice for a discovery of dark matter if the detection were sufficiently compel-ling. The situation for high-energy particle astrophysics is somewhat different, in that it is essential to synthesize data from multiple sources. Cosmic-ray data establish the existence of protons and heavier ions accelerated to extreme energies, but provide little information about the sites of such acceleration because of deflection by Galactic magnetic fields. In contrast,

data from the electromagnetic spectrum identify sources and establish the presence of energetic electrons, but do not provide definitive evidence for or against the presence of energetic baryons. The main processes contributing to the understanding of high-energy particle astrophy-sics include: Cosmic rays, which demonstrate the existence of astrophysical particle accelerators capable of accelerating protons to energies in excess of 10^{20} eV. Radio emission, which is clearly non-thermal in origin and requires the presence of relati-vistic electrons and a significant magnetic field. High-energy photon emission (X-rays and soft gamma rays), which is highly correlated with radio emission and implies similar source properties. High-energy gamma rays, which require higher-energy electrons than radio and X-ray emission. High-energy neutrinos, which must be produced via secondary interactions of high-energy baryons. In this chapter, we provide a clear theoretical background to emissions of particles, lifetime of radiating electrons, energy loss mechanisms, and acceleration mechanisms of cosmic ray electrons, which are vital for radio halo generation in clusters with magnetic fields of a few μG. The primary process at the origin of radio emission in the universe is the synchrotron process. Its spectral and polarization properties provide important information on the physics and evolution of radio sources. Radio emissions from AGNs and the ICM are caused by synchrotron radiation, produced by the spiraling motion of relativistic electrons in a magnetic field. The emitted power depends on the electron's energy γ and the magnetic field strength. The principal emission mechanisms at radio or microwave wavelengths are arranged approximately in increasing order of wavelength. Thermal emission from dust The plane of our Galaxy contains warm dust at temperatures of around 10–30 K. The thermal radia-tion from this material lies primarily in the far-infrared or sub-millimeter bands. Thermal emission from the early universe CMB. The peaks at longer wavelengths than the radiation from warm dust. Spinning dust AME occurs in the frequency range 10–60 GHz and is believed to be emitted by rapidly-spinning dust grains. Line emission from gas The 21 cm line of neutral hydrogen is the most famous radio spectral line, important for studying the chemistry of molecular clouds. Bremsstra-hlung (free-free emission) This radiation

is emitted when an electron loses energy in an interaction with an ion, typically occurring in ionized gases. Synchrotron radiation Emitted by highly relativistic electrons gyrating in a magnetic field, this is the dominant source of astrophysical radio emission at low frequencies [9, 1].

2.2 Synchrotron Radiation

Synchrotron emission is produced by the spiraling motion of relativistic electrons in a magnetic field. The power emitted by a relativistic electron depends on its energy and the magnetic field strength. Higher magnetic field strength requires lower electron energy to produce emission at a given frequency. Relativistic electrons in a uniform magnetic field produce linearly polarized radiation, with the electric (polarization) vector perpendicular to the projection of the magnetic field onto the plane of the sky. The intrinsic degree of polarization depends on the particle energy distribution, typically around $75\% - 80\%$ for common spectral index values. However, complex and disordered magnetic field structures can decrease the obser-ved degree of polarization. The total energy content in a synchrotron radio source consists of contributions from relativistic particles (electrons and protons) and from magnetic fields, considering the fraction of the source volume occupied by magnetic fields (the filling factor). The corresponding magnetic field is referred to as the equi-partition valueB_{eq}. Recent evidence suggests the existence of large-scale diffuse radio sources of synchrotron origin within galaxy clusters, which lack optical counterparts and have no obvious connection to cluster galaxies. The first diffuse radio source detected was the giant radio halo at the center of the Coma cluster, with extended emission later observed at the periphery of the Coma cluster and at the center of the Perseus cluster. Currently, diffuse radio emission with surface brightness down to $0.1\,\mathrm{Jy\,arcsec^{-2}}$ at $1.4\,\mathrm{GHz}$ is known in about 80 clusters, under various evolutionary conditions (merging and relaxed clusters), and across different locations (center, periphery, and intermediate distances) and

size scales (100 kpc to > Mpc). Diffuse sources are typically categorized into halos, relics, and mini-halos, based on their location within the cluster and cluster type (merging or cool-core). These classes will be discussed in subsequent sections. Synchrotron radiation, which results from the emission of very relativistic and ultra-relativistic electrons gyrating in a magnetic field, dominates much of high-energy astrophysics. Synchrotron radiation is responsible for radio emission from the Galaxy, Supernova remnants, and extra-galactic radio sources, as well as for non-thermal optical and X-ray emissions observed in quasars. The term "non-thermal" is frequently used in high-energy astrophysics to describe the emission of high-energy particles[1]. In diffuse cluster radio sources, synchrotron radiation is related to the number density of relativistic electrons, the intensity of the magnetic field, and the power-law with a spectral index related to the electron energy distribution, given by:

$$\beta = \frac{p-1}{2}, \tag{2.1}$$

Typical observed radio spectra show values around $70\% - 80\%$ consistent with $p = 2.5$. Energy losses of the radio-emitting particles lead to changes in the overall energy distribution over time, which modifies the emitted radio spectrum. The polarization of radiation from a population of relativistic electrons in a uniform magnetic field is linear, with the electric (polarization) vector perpendicular to the projection of the magnetic field onto the sky. Synchrotron radiation is the electromagnetic radiation emitted when charged particles, typically electrons, are accelerated in a magnetic field. This phenomenon is particularly significant in astrophysical contexts, such as in the vicinity of neutron stars, pulsars, and active galactic nuclei.

2.2.1 Lorentz Force

The motion of a charged particle in a magnetic field is governed by the Lorentz force, which is described by the following equation:

$$\mathbf{F} = q(\mathbf{E} + \mathbf{v} \times \mathbf{B}), \tag{2.2}$$

where:q is the charge of the particle, E is the electric field, v is the velocity of the particle, and B is the magnetic field. This force is responsible for the acceleration of charged particles within electromagnetic fields, leading to various dynamical behaviors crucial in astrophysical contexts.

2.2.2 Circular Motion in a Magnetic Field

When a charged particle moves perpendicular to a uniform magnetic field, it experiences a magnetic force that causes it to undergo circular motion. The radius r of this motion can be expressed as:

$$r = \frac{mv}{qB}, \tag{2.3}$$

where: m is the mass of the particle, v is the velocity of the particle, and B is the strength of the magnetic field. This relation highlights how the radius of the circular path depends on the particle's mass, charge, velocity, and the magnetic field strength.

2.2.3 Larmor Radiation

A charged particle undergoing circular motion radiates energy in the form of electromagnetic waves, a phenomenon known as Larmor radiation. The power radiated by a non-relativistic charged particle is given by Larmor's formula:

$$P = \frac{2}{3}\frac{q^2a^2}{c^3}, \tag{2.4}$$

where a is the centripetal acceleration. For a particle in circular motion, the centripetal acceleration can be expressed as:

$$a = \frac{v^2}{r}, \tag{2.5}$$

This radiation is significant in astrophysical settings, contributing to the energy loss of charged particles in magnetic fields.

2.2.4 Relativistic Effects

For relativistic particles, where velocities approach the speed of light, the radiation characteristics change dramatically. The mass of the particle is replaced by the

relativistic mass:

$$m = m_0\gamma, \tag{2.6}$$

where $\gamma = \frac{1}{\sqrt{1-\beta^2}}$ and $\beta = \frac{v}{c}$. The power radiated in the relativistic case is expressed as:

$$P = \frac{2}{3}\frac{q^2B^2\gamma^4}{c}, \tag{2.7}$$

This shows that higher energy particles radiate more power, which is crucial for understanding high-energy astrophysical phenomena.

2.2.5 Frequency Spectrum

The frequency of the emitted radiation can be approximated by:

$$\nu = \frac{3}{2}\frac{qB}{2\pi m}\gamma^2, \tag{2.8}$$

This frequency increases with the Lorentz factor γ, indicating that higher-energy particles emit radiation at higher frequencies. The relevance of synchrotron radiation extends to emissions from cosmic rays, supernova remnants, and active galactic nuclei. It is utilized for advanced imaging techniques and materials research. Understanding synchrotron radiation is essential for interpreting various cosmic phenomena and for developing cutting-edge scientific tools.

2.3 Inverse Compton Scattering

In the presence of a magnetic field, relativistic electrons can emit radiation through synchrotron processes as well as through inverse Compton scattering. Inverse Compton scattering describes the process where a high-energy electron transfers part of its energy to a low-energy photon, consequently increasing the photon's energy.

Rate of Energy Transfer

The rate at which energy is transferred from electrons to photons during inverse Compton scattering can be quantified using the Thomson cross section σ_T. This

cross section characterizes the likelihood of scattering events between photons and electrons.

The energy gain per unit time for an electron due to inverse Compton scattering is given by:

$$\frac{dE}{dt} = \frac{4}{3}\frac{\sigma_T}{m_e c} n \gamma^2 E, \tag{2.9}$$

where, n is the number density of the low-energy photons, m_e is the mass of the electron, c is the speed of light, $\gamma = \frac{1}{\sqrt{1-\beta^2}}$ is the Lorentz factor of the electron, and $\beta = \frac{v}{c}$ is the velocity of the electron relative to the speed of light. This equation indicates that the energy gain for an electron is proportional to the square of the Lorentz factor γ, the number density n of the low-energy photons, and the Thomson cross section.

Energy of the Scattered Photon

The energy of the scattered photon E' after interaction with the electron can be expressed as:

$$E' = \gamma^2 E(1 + \beta \cos\theta), \tag{2.10}$$

where: E' is the energy of the scattered photon, E is the initial energy of the photon, γ is the Lorentz factor of the electron, β is the velocity of the electron relative to the speed of light, and θ is the angle between the direction of the incoming photon and the velocity of the electron. This equation highlights how the energy of the photon is modified not only by the Lorentz factor but also by the angle of scattering, indicating that photons can gain significant energy when interacting with high-velocity electrons.

Energy Density of Radiation Field

The energy density U of the radiation field can be expressed as:

$$U = \frac{4}{3}\frac{E^4}{c^3}, \tag{2.11}$$

This formula relates to the energy density of the photon field that interacts with the relativistic electrons. A higher energy density indicates a greater number of

photons available for scattering, which can enhance the overall energy transfer during the inverse Compton process. Inverse Compton scattering is significant in various astrophysical contexts. It enhances the energy of photons and plays a crucial role in the emissions observed from various cosmic sources, such as active galactic nuclei, supernova remnants, and the cosmic microwave background. This process is essential for interpreting high-energy astrophysical phenomena and the behavior of cosmic rays.

2.4 Diffusion Models

Diffusion models are essential for understanding how charged particles, such as cosmic rays, propagate through a magnetic field in astrophysical environments. These models provide insight into the dynamics of particle interactions, energy loss mechanisms, and the resulting emissions observed in the universe.

2.4.1 Diffusion Coefficients

The diffusion coefficient (D) quantifies how easily charged particles spread through a magnetic field. It is a critical parameter that determines the rate of diffusion and is influenced by various factors, including the energy of the particles and the characteristics of the magnetic field. The diffusion coefficient is given by the equation:

$$D = D_0 \left(\frac{E}{E_0} \right)^{\delta}, \tag{2.12}$$

where; D_0 is a normalization constant that sets the scale of diffusion, E is the energy of the particles, which affects their interaction with the magnetic field, E_0 is a reference energy that serves as a baseline for comparison, and δ is the spectral index, typically ranging from 0.3 to 0.6, indicating how diffusion varies with energy. The spectral index δ is particularly important because it reflects the underlying physical processes governing the diffusion of particles. A higher spectral index suggests that diffusion becomes less efficient at higher energies.

2.4.2 Propagation through the Magnetic Field

Charged particles experience scattering due to irregularities in the magnetic field. This scattering results in a random walk process, which can be mathematically described by the diffusion equation:

$$\frac{\partial N}{\partial t} = D\nabla^2 N - \text{loss terms}, \tag{2.13}$$

where: N is the particle density, representing the number of particles per unit volume, D is the diffusion coefficient, which influences how quickly particles spread, $\nabla^2 N$ is the Laplacian operator applied to the particle density, indicating how the density changes spatially, and The term $-$loss terms accounts for processes that reduce the number of particles, such as energy losses or escape from the region of interest. This equation highlights the interplay between particle diffusion and energy loss, which is crucial for understanding the behavior of cosmic rays in various environments, such as supernova remnants or the interstellar medium.

2.4.3 Energy Loss Mechanisms

The overall energy loss for a particle is described by the following equation:

$$|\dot{E}| = |\dot{E}_{\text{sync}} + \dot{E}_{\text{IC}}|, \tag{2.14}$$

where; $|\dot{E}_{\text{sync}}|$ represents the energy loss due to synchrotron radiation, a process where charged particles emit radiation while spiraling in a magnetic field, $|\dot{E}_{\text{IC}}|$ represents the energy loss due to inverse Compton scattering, where high-energy electrons transfer energy to lower-energy photons. Understanding these energy loss mechanisms is essential for modeling the cooling processes of cosmic rays. The cooling time for the particles can be derived from the total energy loss rate:

$$t_{\text{cool}} = \frac{E}{|\dot{E}|} \approx \frac{6\pi m_e c}{\sigma_T B^2}, \tag{2.15}$$

This equation indicates how long it takes for a particle to lose energy, which is crucial for predicting the evolution of cosmic ray populations over time. Understanding the diffusion of charged particles through magnetic fields provides valuable insights into the distribution and behavior of cosmic rays. The structure and strength

of the magnetic field significantly influence both the diffusion processes and energy losses, which in turn affect astrophysical observations. By employing diffusion models and assessing energy loss mechanisms, we gain a deeper understa-nding of how charged particles interact with the galactic magnetic field. This knowledge enhances our comprehension of cosmic ray physics, magnetic field dyna-mics, and the overall processes governing the interstellar medium.

2.5 Methods to Test Results

In this section, we will briefly analyze the study using several key parameters. One of the measurement estimates used in our analysis is the spectral index, defined as $\alpha = 0.05$. This parameter is essential for understanding the expected frequency for each bin in our data.

2.5.1 Spectral Index Analysis

The spectral index α is defined in terms of the flux density S at frequency ν:

$$S \propto \nu^{-\alpha}, \tag{2.16}$$

Using $\alpha = 0.05$, we can analyze how the radio emissions change with frequency, which will help in understanding the underlying mechanisms of radio halos in galaxy clusters.

2.5.2 Evolutionary Model

To estimate how the properties of radio halos change with redshift, we consider the evolution index n. We categorize our analysis based on the following conditions:

For $n \leq 0$,

This condition indicates a potential decline or stabilization in the properties of radio halos with increasing redshift. We will analyze the implications for the synchrotron emission and how it may lead to a decrease in intensity or a flattening of the spectrum.

For $n \geq 0$,

Conversely, this condition suggests that the properties of radio halos may increase or remain stable with redshift. This could indicate ongoing particle acceleration processes or magnetic field amplification within the cluster environment. To implement this analysis, we will: Calculate the expected frequency for each bin using the spectral index. Evaluate the radio halo properties under the evolutionary model conditions to determine the impact of redshift on synchrotron emissions. This methodology will allow us to clarify the relationship between radio emissions, the spectral index, and redshift, ultimately contributing to our understanding of the evolution of radio halos in galaxy clusters. The study of charged particle propagation through the galactic magnetic field involves the use of diffusion models and the assessment of energy loss mechanisms, including synchrotron radiation and inverse Compton scattering.

CHAPTER 3

Observation of Diffuse Radio Emission in Galaxy Clusters

3.1 Diffuse Radio Emission

Diffuse radio emission in galaxy clusters is an intriguing phenomenon that provides valuable insights into the physical processes occurring in these vast cosmic structu-res. Diffuse radio emission refers to extended sources of radio waves that are spread over large areas, as opposed to point-like sources such as individual galaxies or AGN. This emission is primarily produced by synchrotron radiation, which occurs when relativistic electrons spiral around magnetic fields. Observations reveal the dynamics and history of cluster mergers, offering insights into the evolution of large-scale structures. The study of diffuse emission aids in understanding the strength and configuration of magnetic fields within galaxy clusters. These observations contribute to the broader understanding of dark matter and baryonic physics, helping to refine cosmological models. Instruments like the VLA, LOFAR, and the SKA are essential for detecting and analyzing diffuse radio emissions. Combining radio observations with X-ray, optical, and infrared data provides a more comprehensive view of the physical processes at play. Detecting diffuse emis-sions requires high sensitivity and resolution due to their faintness compared to point sources. Separating the diffuse emission from other sources of radio waves, such as foreground galaxies or the cosmic microwave background, can be complex. The observation of diffuse radio emission in galaxy clusters is crucial for advancing our understanding of cosmic structure formation, the behavior of dark matter, and

the role of magnetic fields in the universe. As technology advances, particularly with next-generation radio telescopes, our ability to study these phenomena will continue to improve, unveiling new aspects of the cosmos.

3.2 Galaxy Clusters

Galaxy clusters are the largest gravitationally bound systems in the Universe, typically ranging in diameter from 1 to 10 Mpc. They consist of up to hundreds of galaxies, with masses ranging from 10^{13} to $10^{15}\,M_{\odot}$. Only about 20% of the mass is in the form of baryonic matter, composed of hot ionized gas (the ICM, 15%) and condensed matter in galaxies (5%, e.g., stars). Dark matter, which contributes to approximately 80% of the total mass, provides the dominant gravitational potential of any galaxy cluster. Dark matter filaments govern the structure of the Universe on the largest scales, leading to the formation of the cosmic web, where galaxy clusters reside at the nodes or intersections. Galaxy clusters evolve through the accretion of galaxies and merging with smaller or larger groups. Major mergers of galaxy clusters are among the most energetic events in the Universe, with typical collision velocities around $2000\,\mathrm{km\ s^{-1}}$. These events generate shock waves that heat the ICM, injecting turbulence and raising temperatures to 10^{6} to $10^{8}\,\mathrm{K}$. At such high temperatures, the ICM is nearly fully ionized, and thermal bremsstrahlung dominates the emission in the X-ray regime, with integrated luminosities of L_X from 10^{43} to $10^{45}\,\mathrm{ergs\ s^{-1}}$.

3.2.1 Radio Halos

Found in the central regions of galaxy clusters, radio halos are large-scale structures generated by the acceleration of electrons through turbulence in the ICM caused by mergers. They do not have optical counterparts and are extended sources that roughly follow the ICM baryonic mass distribution. The prototypical example is found in the Coma cluster. Radio halos are referred to as Mpc-scale synchrotron emission regions and are thought to be generated by re-accelerated electrons in a

Figure 3.1: Galaxy Clusters [4]

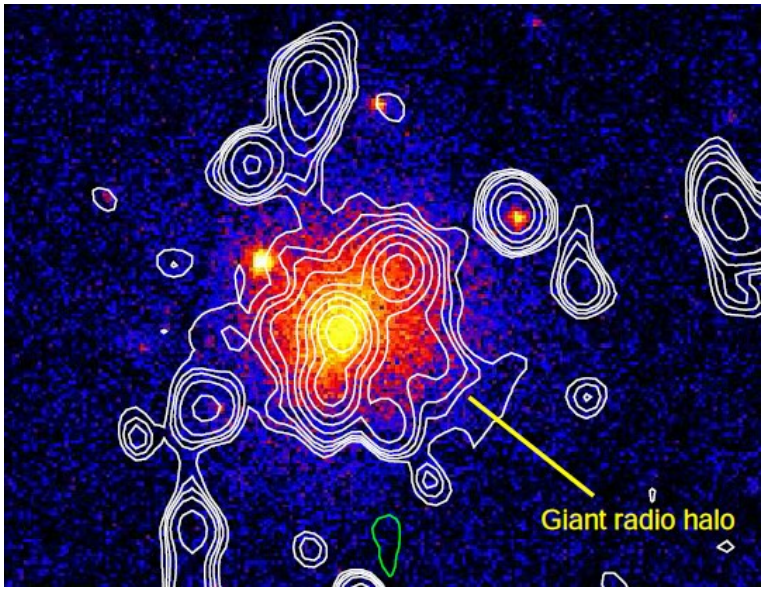

Figure 3.2: Radio Halo [3, 5]

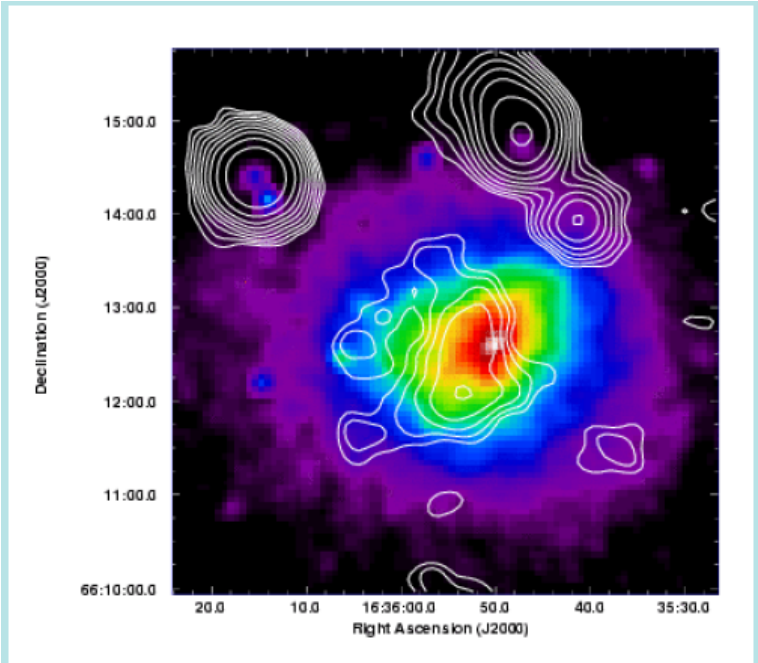

Figure 3.3: Diffuse Radio sources [6, 7]

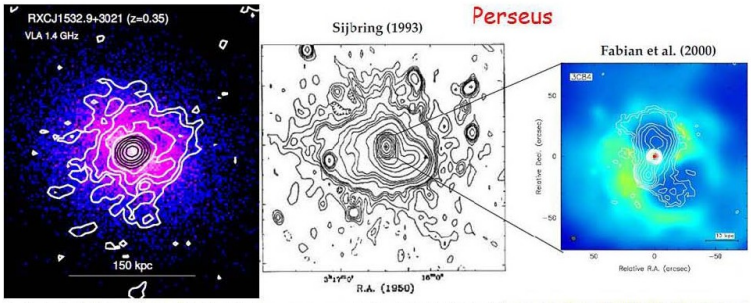

Figure 3.4: Mini halo [8]

cluster's magnetic field. Recent research has indicated a connection between halo occurrence and the cluster's dynamical and environmental properties. Despite significant theoretical advancements, proving halo generation scenarios remains challenging due to the limited number of detected halos [3, 10].

3.2.2 Mini-halos

Radio mini-halos have sizes of approximately 100–500 kpc and are located in relaxed cool core clusters that also host a powerful radio galaxy. They often surround the central galaxies and are associated with star formation activity and feedback from active galaxies. The prototypical mini-halo is found in the Perseus cluster. Unlike radio halos, the synchrotron volume emissivity of mini-halos is generally higher, and the emission directly surrounds the central AGN. Observational difficul-ties persist due to the brightness of central radio galaxies, making it challenging to study mini-halos in detail. However, the number of known mini-halos has been steadily increasing, with the most detailed morphological information available for the Perseus cluster mini-halo.

3.2.3 Relics

Observationally, radio relics are identified by their low surface brightness and steep spectral indices, typically characterized by a spectral index $\alpha > 1$. Their polarized nature is indicative of the magnetic fields present in the surrounding medium. Radio relics are often elongated structures, aligned with the direction of the merger. This morphology is a crucial indicator of their association with shock waves. Observations using radio telescopes like the VLA and the LOFAR have provided detailed images of these structures, revealing their intricate shapes and polarization properties. The formation of radio relics is primarily linked to the re-acceleration of particles by shock waves generated during cluster mergers. These shocks accelerate pre-existing relativistic electrons, leading to synchrotron radiation that can be detected at radio wavelengths. The efficiency of this re-acceleration process is influenced by various factors, including the strength and orientation of

the magnetic fields in the ICM. Theoretical models suggest that the efficiency of electron re-acceleration varies with the properties of the merger event, such as its velocity and the density contrast between the merging clusters. Some studies indicate that relics are more likely to form in off-axis mergers, where the shock geometry allows for effective particle acceleration. Statistical studies of galaxy clusters have shown that relics are found in a variety of environments, including both merging and relaxed clusters. The presence of a relic often correlates with the dynamical state of the cluster, with a higher likelihood of detection in dynamically active systems. Recent surveys have reported that relics are present in approximately 20-30% of merging galaxy clusters. This prevalence highlights their significance as indicators of merger activity and the associated physical proce-sses in the ICM. Future research on radio relics will benefit from advancements in observational techniques and new facilities such as the SKA. These developments will enhance our ability to detect fainter relics and study their properties in greater detail. Further theoretical work is also needed to refine models of particle acceleration in the ICM, particularly in relation to the specific conditions present during cluster mergers. Understanding the role of magnetic fields and turbulence in the environment will be crucial for interpreting observations of relics and their formation mechanisms. Therefore, Radio relics serve as important probes of the physical processes occurring in galaxy clusters. Their study not only enhances our understanding of cluster dynamics and merger histories but also contributes to our broader knowledge of cosmic structure formation. As observational capabilities improve, we anticipate significant advancements in our understanding of these fascinating cosmic structures. The expected behavior of the correlation is twofold. First, at low redshifts, the observed power may approximate the emitted luminosity. Second, as redshift (z) increases, the observed power $P(z)$ typically decreases due to the effects of increased distance and cosmic expansion. Examining the selected data on redshift (z) and power ($\log P(1.4)$), the values range from $z = 0.023$ (representing a nearby cluster) to $z = 0.307$ (indicating a more distant cluster). This range allows us to investigate how the properties of radio halos evolve as we look back

in time. The power values ($\log P(1.4)$) predominantly hover around 24, with occasional instances of 23 and 25. This consistency suggests that radio emissions from the halos do not vary dramatically across this redshift range, at least within the observed clusters. Most clusters exhibit stable power outputs, indicating that the mechanisms driving radio emissions remain relatively constant over this range of redshifts. The slight deviations in power (from 23 to 25) may indicate subtle differences in halo properties, such as magnetic field strength or electron density, which could influence the emitted synchrotron radiation. The observed stability in power across varying redshifts implies that the physical processes involved in halo formation and maintenance are robust over time. Clusters formed early in the universe may continue to produce similar radio emissions as they evolve, which is crucial for understanding the lifecycle of such structures. The lack of significant variation in power suggests that the underlying physics governing radio halo emissions is largely independent of redshift, at least within the observed range. This provides insights into the conditions of the early universe and their relation to current observations. The analysis of redshift and power values reveals important aspects of radio halos in galaxy clusters. The stability in power suggests a robust mechanism at work, potentially offering a window into the processes governing galaxy cluster evolution across cosmic time. Future research could further elucidate these relationships and contribute to our understanding of the universe's structure and evolution.

3.3 Statistical Analysis of Radio Halos

The statistical analysis of radio halos is crucial for understanding their prevalence, properties, and the physical processes governing their formation. This section outlines the methodologies used for the analysis, presents the results, and discusses their implications.

Name	z	kpc	$S(1.4)$ mJy	$LogP(1.4)$ W/Hz	LLS Mpc	$Lx(10^44)$ erg/sec	$M500(10^{14})M_{\odot}$
A1656	0.023	0.5	530	24	0.8	4	
A1213	0.047	0.9	72	24	0.2	0.1	
A3562	0.049	1	20	23	0.3	1.6	
A754	0.054	1	86	24	1	2	
A2319	0.056	1	153	24	1	8.5	
A2256	0.058	1	103	24	0.8	3.8	
CL0217+70	0.066	1	59	24	0.7	0.6	
A399	0.072	1	16	23	0.6	3.8	
A401	0.074	1	17	23	0.5	6.5	
A2255	0.081	2	56	24	0.9	2.6	
A523	0.104	2	59	24	1	1.1	
RXJ0107.7+5408	0.107	2	55	24	1	5.4	
A2034	0.113	2	14	24	0.6	3.8	
A2294	0.128	3	6	24	0.5	3.9	
A545	0.154	3	23	24	0.9	5.6	
A2218	0.176	3	5	24	0.4	5.8	6.41
A2254	0.178	3	34	24	0.9	4.6	
A665	0.182	3	43	25	2	9.7	8.23
A1689	0.183	3	10	24	0.7	12	8.86
A520	0.199	3	34	25	1	8.3	7.06
A2163	0.203	3	155	25	2.3	22.7	16.44
A773	0.217	4	13	24	1.3	8	7.08
RXCJ1514.4-1523	0.220	4	10	24	1.5	7.2	8.34
A2219	0.226	4	81	25	1.7	12.2	11.01
A746	0.232	4	18	25	0.9	3.7	
RXCJ1314.4-2515	0.244	4	20	25	1.6	10.8	6.15
A521	0.253	4	5.9	24	1.2	8.5	6.91
A1758a	0.279	4	16.7	25	1.5	7.1	7.99
A697	0.282	4	5.2	24	0.7	10.4	11.48
IE0657-56	0.296	4	78	25	2	22.6	
A781	0.300	4	21	25	1.6	4.6	
A521	0.253	4	5.9	24	1.2	8.5	6.91
A1758a	0.279	4	16.7	25	1.5	7.1	7.99
A697	0.282	4	5.2	24	0.7	10.4	11.48
IE0657-56	0.296	4	78	25	2	22.6	
A781	0.300	4	21	25	1.6	4.6	
A1300	0.307	5	20	25	1.3	13.7	8.83

Table 3.1: The number of radio Halos collected from current work [1, 2]

3.3.1 Data Collection

The data for this analysis were collected from a variety of surveys that reported on the properties of radio halos and relics in galaxy clusters. The data was solely gathered for 31 halos recorded using parameters such as: Redshift (z): Provides information on the distance and age of the cluster. Spectral Index (α): Indicates the steepness of the radio spectrum, with lower values suggesting stronger emissions at higher frequencies. Radio Power ($P_{1.4}$): Measured at 1.4 GHz, this is a critical parameter for understanding the energy output of the halos. X-ray Luminosity (L_x): Offers insights into the thermal properties of the ICM and is indicative of cluster mass. Size (LLS): Linear size of the radio emission, which correlates with the dynamical state of the cluster.

3.4 Data Analysis and Interpretation

3.4.1 Observed Frequencies of Halos in Galaxy Clusters

The following table summarizes the number of halos in cluster galaxies counted in each redshift bin:

Redshift Bin	**Number of Halos**	**Percent of Each**
Bin 1: $z \leq 0.1$	10	32.26%
Bin 2: $0.1 < z \leq 0.2$	10	32.26%
Bin 3: $0.2 < z \leq 0.3$	10	32.26%
Bin 4: $z > 0.3$	1	3.22%

If the null hypothesis is rejected, we conclude that there is a significant difference in the distribution of galaxies across the redshift bins. If the null hypothesis is not rejected, we conclude that the distribution of galaxies is consistent with the expected frequencies.

Assuming the null hypothesis is true, the expected frequency for each bin (E_i) can

be calculated based on the overall distribution. If we assume a uniform distribution:

$$E_i = \frac{N}{k} = \frac{31}{4} = 7.75, \tag{3.1}$$

where k is the number of bins (in this case, $k = 4$).

The chi-squared statistic (χ^2) is calculated using the formula:

$$\chi^2 = \sum \frac{(O_i - E_i)^2}{E_i} = 6.532, \tag{3.2}$$

where O_i is the observed frequency and E_i is the expected frequency for each bin.

The degrees of freedom (df) for the test can be calculated as:

$$df = k - 1, \tag{3.3}$$

For our case, we use a chi-squared distribution table to find the critical value for df at a chosen significance level (commonly $\alpha = 0.05$). According to the decision rule, if χ^2 > critical value, the null hypothesis is rejected.

The first three bins ($z \leq 0.1$, $0.1 < z \leq 0.2$, and $0.2 < z \leq 0.3$) each contain 10 halos, accounting for approximately 32.26% of the total halos observed. This indicates a consistent presence of halos in the lower redshift range, suggesting that cluster galaxies in these epochs are more numerous or more detectable. In contrast, Bin 4 ($z > 0.3$) has only 1 halo, which represents 3.22% of the total. This sharp decline in the number of halos at higher redshifts suggests that fewer halos are being formed or detected in this range.

The observed frequencies of halos in cluster galaxies suggest a trend where the number of detectable halos decreases with increasing redshift. The consistent counts in the lower redshift bins imply a stable population of halos, while the sparse detection at higher redshifts indicates potential changes in formation processes or observational challenges. This analysis provides valuable insights into

the evolutionary dynamics of galaxy clusters and the broader implications for our understanding of cosmic structure formation.

3.4.2 Evolution of Radio Halo in Galaxy Clusters

The evolutionary model for estimating how properties of radio halos change with redshift can be expressed using the following parametric equation:

$$P(z) = P_0 \times (1+z)^n, \tag{3.4}$$

Components of the Equation: $P(z)$: Represents the property of interest (e.g., luminosity, surface brightness, or density) at redshift z, P_0: The value of the property at a reference redshift, typically at $z = 0$. This serves as the baseline measurement, $(1+z)^n$: This term describes how the property evolves with redshift, n: The evolution index that indicates the nature of the evolution.

If $n > 0$: The property increases with redshift, suggesting that radio halos become more luminous or dense as we look back in time. If $n < 0$: The property decreases with redshift, indicating a decline in luminosity or density at earlier epochs. If $n = 0$: There is no evolution, meaning the property remains constant across redshifts.

Observations Regarding the Evolution of Radio Halos:

- For $z > 0$ and $n > 0$:
$$P(z) = 24.55,$$
- For $n < 0$ (e.g., $n = -1$):
$$P(z) = 23.46,$$

Positive Evolution ($n > 0$): This indicates that the property $P(z)$ increases with redshift. As we look back in time, the radio halos appear more luminous or prominent. This suggests that processes such as increased star formation or energy injection from AGN in earlier cosmic epochs enhance radio halo luminosity.

Negative Evolution ($n < 0$): This indicates that $P(z)$ decreases with redshift. As z increases, the radio halos appear less luminous or prominent. This suggests that conditions leading to radio halo formation were less favorable at higher redshifts, possibly due to energy dissipation or environmental changes.

The stark difference between cases of $n > 0$ and $n < 0$ highlights the complexity of radio halo evolution. Understanding these trends is crucial for unraveling the history of cosmic structures and the fundamental processes driving their evolution.

3.4.3 Surface Brightness

Cluster	**Surface Brightness**	**Synchrotron Loss**	**IC Loss**	**Total Energy Loss**
A1656	530	3.39×10^{-27}	3.55×10^{-28}	3.74×10^{-27}
A1300	20	3.39×10^{-27}	3.55×10^{-28}	3.74×10^{-27}

When we analyze the diffuse radio emission for the two clusters, A1656 and A1300, using the previously discussed equations and assumptions, we can calculate the surface brightness, energy loss, and cooling time for each cluster. The surface brightness is given directly, but we can relate it to the electron density and magnetic field strength.

Surface Brightness Values:

- A1656: $S(1.4) = 530\,\text{mJy}$
- A1300: $S(1.4) = 20\,\text{mJy}$

3.4.4 Energy Loss for A1656

Assumptions:

- Magnetic Field Strength $B = 1\,\mu\text{G} = 10^{-6}\,\text{T}$
- Average Energy of Electrons $E \approx 1\,\text{GeV}$ ($\gamma \approx 2000$)

Energy Loss Calculations: (Synchrotron Radiation Loss)

$$\dot{E}_{\text{sync}} = \frac{4}{3}\sigma_T \frac{B^2}{\mu_0}\gamma^4, \tag{3.5}$$

Substituting the values:

$$\dot{E}_{\text{sync}} = \frac{4}{3}(6.65 \times 10^{-29}) \left(\frac{(10^{-6})^2}{4\pi \times 10^{-7}} \right) (2000)^4$$

$$\approx 3.39 \times 10^{-27}\,\text{W},$$

Inverse Compton Scattering Loss:

$$\dot{E}_{\text{IC}} \approx \frac{4}{3}\sigma_T U_{\text{photon}} \gamma^2, , \tag{3.6}$$

$$\approx 3.55 \times 10^{-28}\,\text{W},$$

Total Energy Loss eq(2.15):

$$|\dot{E}| = 3.39 \times 10^{-27} + 3.55 \times 10^{-28} \approx 3.74 \times 10^{-27}\,\text{W},$$

Cooling time For A1656:

$$t_{\text{cool}} = \frac{E}{|\dot{E}|} = \frac{1.6 \times 10^{-10}}{3.74 \times 10^{-27}} \approx 4.28 \times 10^{16}\,\text{s} \approx 1.36 \times 10^{9}\,\text{years}, using, eq(2.16)$$

Energy loss For A1300:

Synchrotron Radiation Loss: Using the same magnetic field and energy assumptions:

$$\dot{E}_{\text{sync}} \approx 3.39 \times 10^{-27}\,\text{W}, \quad \text{(same as A1656)},$$

Inverse Compton Scattering Loss:

$$\dot{E}_{\text{IC}} \approx 3.55 \times 10^{-28}\,\text{W}, \quad \text{(same as A1656)},$$

Total Energy Loss:

$$|\dot{E}| = 3.39 \times 10^{-27} + 3.55 \times 10^{-28} \approx 3.74 \times 10^{-27}\,\text{W},$$

Cooling time For A1300:

$$t_{\text{cool}} = \frac{E}{|\dot{E}|} = \frac{1.6 \times 10^{-10}}{3.74 \times 10^{-27}} \approx 4.28 \times 10^{16}\,\text{s} \approx 1.36 \times 10^{9}\,\text{years},$$

Diffusion Coefficient

The diffusion coefficient D can be derived from the diffusion equation:

$$\frac{\partial N}{\partial t} = D\nabla^2 N - \text{loss terms}, frome q(2.13)$$

Here, D quantifies how quickly particles spread due to scattering. The energy loss terms (synchrotron and inverse Compton losses) can influence the diffusion coefficient. The total energy loss can provide insight into how particles diffuse over time. If you have the total energy loss P_{total} and the density of particles N, you can estimate D using the form:

$$D \approx \frac{P_{\text{total}}}{N \cdot \text{cooling time}}, \tag{3.7}$$

For example, using the data from the table for cluster A1656: - Total Energy Loss $P_{\text{total}} = 3.74 \times 10^{-27}$ W - Cooling Time $t_{\text{cool}} = 1.36 \times 10^{9}$ years $\approx 4.29 \times 10^{16}$ seconds (conversion: 1 year $\approx 3.15 \times 10^{7}$ seconds). Assuming you have the particle density N for the cluster, you can plug in the values to estimate D. If you don't have N, you might need to derive it based on observations or additional data. Assuming N is known (for example, $N = 1 \times 10^{-3}$ m^{-3}), the diffusion coefficient can be estimated as follows:

$$D \approx \frac{3.74 \times 10^{-27}\,\text{W}}{(1 \times 10^{-3}\,\text{m}^{-3}) \cdot (4.29 \times 10^{16}\,\text{s})},$$

Calculating D:

$$D \approx \frac{3.74 \times 10^{-27}}{4.29 \times 10^{13}} \approx 8.70 \times 10^{-41}\,\text{m}^2/\text{s},$$

We estimate the diffusion coefficient based on energy loss and cooling time. If we have specific values for particle density N, we can refine this calculation accordingly. A1656 has a surface brightness of 530 mJy, while A1300 has a much lower value of 20 mJy. This significant difference indicates that A1656 has a

much stronger radio halo, suggesting a higher density of relativistic electrons or a stronger magnetic field. The higher surface brightness in A1656 could be attributed to ongoing proces-ses, such as active star formation or interactions between cluster members, which contrib-ute to the generation of relativistic electrons.

Energy Loss Mechanisms:

Both clusters show similar rates of energy loss due to synchrotron radiation and inverse Compton scattering. The synchrotron loss is the dominant mechanism, indicating that the primary source of radio emission in both clusters is the synchrotron radiation from relativis-tic electrons spiraling in the magnetic field. The total energy loss for both clusters is approximately 3.74×10^{-27} W. This consistent value across both clusters suggests that, despite the differences in surface brightness, the mechanisms for energy loss are similar. This might imply that the conditions (magnetic field strength, electron density) in both clusters are comparable, but the overall environment in A1656 is more conducive to generating higher surface brightness. The cooling time for both clusters is estimated at approximately 1.36 billion years (1.36×10^9 years). This long cooling time indicates that the relativistic electrons can sustain their energy and contribute to radio emission for a significant period. If new electrons are continuously injected into the system (e.g., from supern-ova remnants or active galactic nuclei), the radio halos in both clusters can persist over cosmological times-cales. The cooling time being similar for both clusters suggests that, while A1656 has a stronger radio emission, its relativistic electron population is not experiencing a faster rate of energy loss compared to A1300. The analysis of the diffusion coefficient D based on the data from clusters A1656 and A1300 provides valuable insights into the behavior of charged particles in astrophysical environments. A summary of data interpretation expresses that: The diffusion coefficient quantifies how quickly particles spread in a medium due to random scattering processes. In astrophysical contexts, this is crucial for

the transport of cosmic rays and other charged particles in the presence of magnetic fields. The total energy loss (both synchrotron and inverse Compton losses) reflects the interactions of charged particles with their environment. High energy loss rates imply that particles are losing energy rapidly, which can affect their mobility and diffusion. Caused by charged particles spiraling in magnetic fields, leading to radiation emis-sion. When high-energy particles transfer energy to low-energy photons, resulting in increased photon energy. The total energy loss in clusters A1656 and A1300 indicates that particles are undergoing significant energy dissip-ation, which can hinder their ability to diffuse freely through the medium. The calculated cooling time of approximately 1.36×10^9 years indicates how long it takes for particles to lose a significant portion of their energy through these processes. A longer cooling time suggests that while particles are losing energy, they can still travel considerable distances before they significantly lose their kinetic energy. The estimated diffusion coefficient $D \approx 8.70 \times 10^{-41}$ m^2/s is quite small, indicating that the diffusion of charged particles in these clusters is relatively slow. This can be interpreted in the following ways: The low value of D suggests that particles may be trapped in certain regions of the magnetic field, leading to reduced mobility. This could be due to strong magnetic fields or irregularities in the magnetic structure that create barriers to diffusion. The slow diffusion rate implies that cosmic rays may take a long time to spread throughout the cluster environment, affecting observations of high-energy emissions and the overall dynamics of cosmic ray popul-ations. The discussion highlight the complex interplay between the mechanisms generating diffuse radio emissions in galaxy clusters. A1656's higher surface bright-ness may point to a more dynamic environment, possibly influenced by recent cluster mergers or active galactic nuclei. Understanding these emissions is crucial for studying cosmic structure formation and the role of magnetic fields in cluster dynamics. Future observations, especially at different frequencies, could help refine these interpretations and provide deeper insights into the physical processes at play. We utilized observational data from various framework and researches, to gather information on radio halos and their properties

across different galaxy clusters. The data was analyzed statistically using theoretical methods and enabled to comp-are with images images captured in many other surveys. And we employed diffusion models to understand how charged particles propagate through the galactic magnetic field. This involved calculating the diffusion coefficients and assessing energy loss mechanisms, including synchrotron radiation and inverse Compton scattering. The results of the diffusion models were compared with observational data to validate the theoretical predictions regarding particle behavior and energy loss. We analyzed the radio spectrum of halos by fitting observational data to theoretical models. This included measuring the (α) to characterize the emission properties of each halo. The spectral indices were correlated with other cluster properties, such as temperature and X-ray luminosity, to explore the relationships between different physical parameters. We performed statistical analysis to examine the distribution of radio luminosity among different galaxy clusters, categorizing them into relaxed and disturbed clusters. High-resolution imaging techniques were empl-oyed to analyze the morphologies of radio halos, allowing us to identify peculiar structures and features influenced by turbulence within the ICM. Observed morphol-ogies were compared with theoretical predictions from simulations to identify discre-pancies and areas for further investigation. The methodologies were integrated to create a comprehensive framework for understanding the dynamics of radio halos. Observational data informed the diffusion modeling, while spectral and morphological analyses provided context for the statistical findings. This structured outline clearly describes the methodologies used in your study and how they were integrated, providing a comprehensive overview of your research approach.

CHAPTER 4

Primary electron model

4.1 Origin of relativistic particles

The origin of relativistic particles in radio halos and the mechanisms transferring energy from the ICM into the relativistic electron population have been developed. Observations reveal that clusters with radio emission are characterized by powerful dynamical activity due to merging processes. These clusters are identified by substructures and distortion in the X-ray brightness distribution; temperature gradients and gas shocks; absence of a strong cooling core; and a larger distance from the nearest neighbors compared to clusters with similar X-ray luminosity. Some mergers appear more isolated, leading to a depletion of the nearest neighbors. The electrons responsible for the diffuse radio emission can be either primary or secondary electrons. One of the main open questions for the re-acceleration model is the source of electrons. Several possibilities arise, including proton-proton interactions being an obvious candidate with secondary electrons. They could also have been previously accelerated at cluster mergers and increased shocks. A third possibility is that primary relativistic electrons in the cluster volume were provided by AGN activity (quasars, radio galaxies, etc.), or by star formation in normal galaxies (supernovae, galactic winds, etc.) during the cluster's dynamical history. AGN is becoming increasingly evident due to low-frequency observations. These electrons suffer significant energy loss mainly because of synchrotron and inverse Compton emission, thus re-acceleration is required to keep their energy at levels essential to produce the observed synchrotron radio emission in weak magnetic fields. For

these reasons, primary electron models can also be referred to as re-acceleration models. The origin of diffuse radio sources has been historically debated between two models: the hadronic and re-acceleration model. In the hadronic model, radio-emitting electrons are produced in hadronic interactions between CR protons and ICM protons. In the re-acceleration model, electrons are re-accelerated during powerful states of ICM turbulence, as a consequence of cluster merger events. The statistical distribution of spectral indices of radio halos, ranging from very uniform to variable, might provide good tests for the turbulent re-acceleration model. Spectral cutoffs in the model have been observed rarely. Measurements would be better through single-dish observations for the analysis of diffuse emission.

4.1.1 Re-acceleration by turbulence

There are two main ways that change the transfer of energy from the cluster ICM to the radiating particles: cluster turbulence and shocks. In this chapter, we discuss solely radio halo sources. Turbulent re-acceleration is thought to be the main mechanism responsible for generating radio halos.During cluster mergers, turbulence is generated throughout the cluster over Mpc scales. Thus, energy can be transferred from the ICM into the non-thermal component through resonant or non-resonant interactions of electrons with MHD turbulence. Direct measurements of the ICM have so far only been performed for the Perseus cluster with the Hitomi satellite, finding a line-of-sight velocity dispersion of 164 ± 10 km s^{-1}. Future measurements with XRISM, LOFAR, and Athena will provide important tests on the turbulent motions in halo and non-halo hosting clusters for the turbulent re-acceleration model. Turbulence induced by major cluster mergers indicates giant radio halos, while in the cluster cores generated by gas disturbances would indicate mini-halos.

4.1.2 Re-acceleration by shocks

In the theory of primary electron models, merger shocks can accelerate relativistic electrons to produce large-scale synchrotron radio emission. However, the radiative lifetime of the emitting electrons diffusing away from these shocks is so short that they would only be able to produce relics and not Mpc-sized spherical radio halos. Additionally, several papers have recently pointed out that the Mach number of typical shocks produced during major merger events is too low to generate non-thermal radiation with the observed fluxes, spectra, and statistics. Shock acceleration is a first-order Fermi process of great importance in radio astronomy, recognized as the mechanism responsible for particle acceleration in supernova remnants. The acceleration occurs diffusively, with particles scattering back and forth across the shock, gaining energy at each crossing proportional to their energy. The acceleration efficiency is mostly determined by the shock Mach number. The magnetic field within the relic is aligned with the shock front, and the radio spectrum is flatter at the shock edge, where the radio brightness is expected to decline sharply. These expectations are consistent with the classic elongated structure of relics, almost perpendicular to the merger axis, and their polarization properties. Unlike radio halos, cluster radio shocks can be associated with specific cluster regions where a shock wave is present or where a shock wave recently passed. The detection of shocks in the ICM is observationally challenging. Therefore, the classification will remain uncertain for some sources. However, for several sources, the presence of a shock at their location has been confirmed by X-ray observations, which we argue supports the creation of a radio shock class. Thus, the term radio shock could be classified as large radio relics, Gischt, and double relics, whereas AGN fossil plasma is re-accelerated at a large cluster merger shock.

4.2 Halo Observations

Our observations may primarily capture the brightest regions of halos, potentially missing extended outer areas that exhibit very low surface brightness. These missed regions are insufficient to account for significant deficiencies in radio power. The observed halo radio power is likely influenced by ongoing major mergers within the clusters and the evolutionary history of the cluster over longer timescales. Some evidence supports the idea that the merger fraction increases significantly starting at $z = 0.4$. Others confirm significant evolutionary changes in clusters over time, reinforcing the hypothesis about the factors influencing radio power.

4.2.1 Redshift and Power in Galaxy Clusters

The luminosity distance (D_L) as a function of redshift (z) is given by:

$$D_L(z) = \frac{(1+z) \cdot D_C(z)}{H_0}, \tag{4.1}$$

where $D_C(z)$ is the comoving distance and H_0 is the Hubble constant. The comoving distance can be calculated using:

$$D_C(z) = \int_0^z \frac{c}{H(z')}\, dz', \tag{4.2}$$

Here, $H(z)$ is the Hubble parameter at redshift z, and c is the speed of light. The relationship between the emitted luminosity (L) of a galaxy cluster and the observed flux (F) at redshift z is given by:

$$F = \frac{L}{4\pi D_L^2}, \tag{4.3}$$

Combining these equations, we can express observed power (P) as a function of redshift:

$$P(z) = \frac{L}{4\pi \left(\frac{(1+z)D_C(z)}{H_0}\right)^2}, \tag{4.4}$$

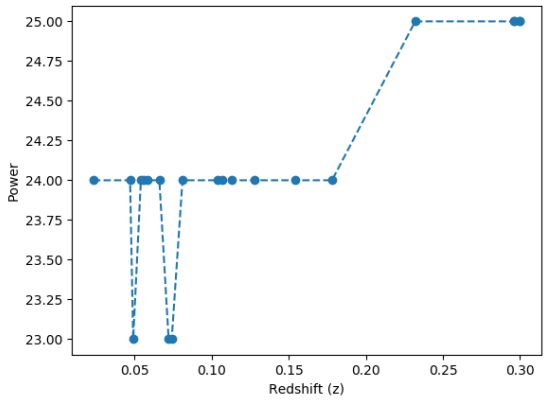

$$P(z) = \frac{1}{z^2+1}$$

Figure 4.1: Redshift vs Power

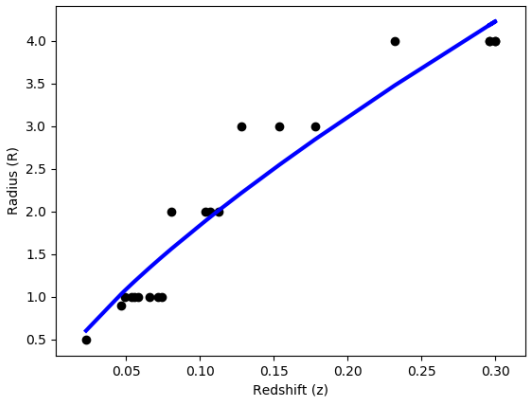

$$L(z) = \frac{L_0}{(1+z)^2}$$

Figure 4.2: Luminosity as a function of redshift

4.2.2 Evolution of Halos

The figure 4.2 likely presents a graph illustrating the relationship between the luminosity distance of astronomical objects and their redshift. The X-axis typically represents redshift (z), which measures how much the wavelength of light has been stretched due to the expansion of the universe. Higher redshift values indicate objects that are further away and possibly older. The Y-axis represents luminosity distance, a measure of how far away an object appears based on its brightness and the effects of distance in an expanding universe. The graph usually shows an increasing trend, where luminosity distance increases with redshift. This reflects the fact that more distant objects appear dimmer and are thus further away. Higher redshift corresponds to earlier times in the universe, suggesting

that the universe has been expanding over time. This relationship is fundamental in cosmology, as it helps in understanding the scale and evolution of the universe. This data is crucial for measuring distances to faraway galaxies, studying the expansion of the universe, and exploring phenomena like dark energy. It is essential in cosmology for determining distances to far-off galaxies and understanding the expansion of the universe. Higher redshifts indicate greater distances and earlier times in the universe. As redshift increases, so does luminosity distance, reflecting the fact that we are observing light that has traveled longer distances over time. The figure typically shows a linear or slightly curved increase in luminosity distance with redshift, aligning with the predictions of an expanding universe. This trend helps confirm models of cosmic expansion and can provide insights into the rate of that expansion, influenced by factors like dark energy. By examining the luminosity distance at various redshifts, researchers can infer how the properties of galaxy clusters, such as their mass and luminosity, evolve over cosmic time. The evolution of clusters from higher redshifts (earlier epochs) to lower redshifts (more recent times) can reveal insights into the processes that govern cluster formation and the role of mergers and interactions. The relationship illustrated in the figure supports the idea that the energy dynamics of radio halos may remain stable over time. This stability suggests that the mechanisms responsible for radio emissions in clusters do not change dramatically as the universe evolves. Investigating how these trends hold at even higher redshifts could enhance our understanding of the early universe and the formation of large-scale structures. The 4.2 figure is a vital tool for interpreting the evolution of galaxy clusters and their radio emissions. It underscores the relationship between distance and light travel time, providing cosmological insights that are crucial for understanding the lifecycle of galaxy structures and the physics governing their emissions. This understanding can inform future studies and refine models of cosmic evolution.

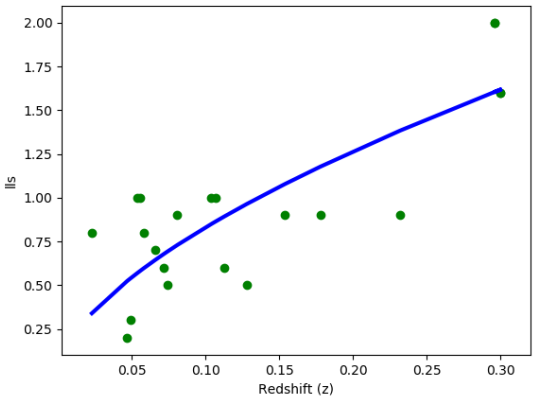

$$L_X(z) = L_{X0} \cdot (1+z)^{\alpha} \; z = \frac{\lambda_{\text{observed}} - \lambda_{\text{emitted}}}{\lambda_{\text{emitted}}}$$

Figure 4.3: The redshift distribution in relation to the X-ray luminosity

4.2.3 Redshift and X-ray luminosity for galaxy clusters

The X-ray luminosity in a merger is a very good indicator of the occurrence of a major merger between high mass systems. The redshift range is much narrower than the group sample with most clusters lying at (z$\leq$ 0.1) and only a few objects reaching ($z \approx 0.3$). X-axis: Redshift (z). It represents how much the light from distant objects has been stretched due to the expansion of the universe. Higher values indicate greater distances and earlier times in the universe. Higher luminosity suggests more energetic and massive clusters, often associated with ongoing or recent mergers. The data suggests that X-ray luminosity is a reliable indicator of major merger events within high-mass galaxy systems. High X-ray luminosity typically correlates with increased energy and temperature in the ICM, which can result from the dynamical activity of merging clusters. The observed redshift values primarily cluster around $z < 0.1$, indicating that most of the analyzed clusters are relatively nearby. A small number of clusters extend to $z \approx 0.3$, suggesting that while significant mergers are ongoing, they are predominantly observed in more recent cosmic times. The concentration of clusters at lower redshifts may imply that major merger activity peaks in the local universe rather than at earlier epochs. This observation contrasts with expectations that high-redshift clusters would show more merger activity due to the higher density of the universe in the past. The relationship between redshift and X-ray luminosity provides insights

into how clusters evolve through mergers over time. High lumin-osity can indicate that a cluster is currently undergoing a merger or has recently merged, influencing its structure and dynamics. The data supports the hypothesis that the mechanisms driving cluster formation and evolution are robust across cosmic time but manifest differently at various redshifts. Clusters formed earlier may have undergone significant merging activity that has shaped their current properties, while more recent mergers may still be influencing nearby systems. The narrow redshift range highlights the need for further studies to observe clusters at higher redshifts to understand the evolution of merger dynamics in the early universe. Investigating the relationship between X-ray luminosity and other prop-erties could provide a more comprehensive understanding of cluster evolution. The interpretation of the redshift distribution in relation to X-ray luminosity reveals important insights into the processes governing the formation and evolution of galaxy clusters. The data suggests that major mergers are primarily occurring in the more recent universe, emphasizing the role of X-ray luminosity as a key indicator of merger activity. This understanding is crucial for refining models of cosmic evolution and for planning future observational campaigns to explore the dynamics of galaxy clusters across different epochs.

4.2.4 Surface brightness

The surface brightness values for the two clusters indicate a significant difference in the intensity of diffuse radio emissions: A1656, with a surface brightness of 530 mJy, A1656 exhibits a strong radio halo. This suggests a dense population of relativistic electrons and/or a stronger magnetic field within the cluster. A1300, in contrast, A1300s surface brightness of 20 mJy suggests a much weaker radio halo. This could indicate a lower density of relativistic electrons or a less intense magnetic field. The higher surface brightness in A1656 may be attributed to ongoi-ng astrophysical processes, such as, the presence of young, energetic stars can accelerate electrons, contributing to synchrotron radiation. Interactions between galaxies in the cluster can generate shocks, further energizing particles and enhan-cing the

radio emission.

4.2.5 Energy Loss Mechanisms

The calculations for synchrotron and inverse Compton scattering losses provide insight into how energy is dissipated in the clusters: The calculated synchrotron radiation loss of $3.39 \times 10^{-27}\,W$ for both clusters indicates the efficiency of the magnetic field in converting kinetic energy of electrons into radiation. The inverse Compton scattering losses of $3.55 \times 10^{-28}\,W$ suggest that the background photon field contributes to the energy loss of the relativistic electrons, particularly in environments with significant radiation fields.

4.2.6 Cooling Time

The cooling time for both clusters is approximately 1.36×10^{9} years. This indicates the relatively long cooling time suggests that the relativistic electrons can remain in the halo for extended periods before losing significant energy. This is indicative of a stable environment where electrons can accumulate and persist as a population. The analysis of the surface brightness, energy loss mechanisms, and cooling times for clusters A1656 and A1300 provides valuable insights into the physical conditions in these environments. The stark contrast in surface brightness between A1656 and A1300 underscores the dynamic and active nature of A1656 compared to the more quiescent state of A1300. This has implications for understanding cluster evolution and the processes driving relativistic particle acceleration. The energy loss calculations highlight the importance of magnetic fields in influencing the behavior of relativistic electrons. A stronger magnetic field in A1656 likely contrib-utes to its enhanced radio emission. The results indicate that A1656 is a more favorable environment for the study of cosmic rays and their interactions, making it a key target for future observational campaigns. Understanding the mechanisms behind the generation of relativistic electrons can shed light on the broader processes at play in galaxy clusters. Further investigations could involve multi-wavelength observations to correlate radio emissions with X-ray and

gamma-ray data, providing a more comprehensive view of particle acceleration processes.

Additionally, numerical simulations could help model the dynamics within these clusters, offering deeper insights into the physical processes at work. In summary, this analysis not only enhances our understanding of individual clusters but also contributes to the broader field of astrophysics by elucidating the connections between particle physics, electromagnetic processes, and cosmic structure formation.

4.2.7 Diffusion Coefficient

Understanding the diffusion coefficient in clusters like A1656 and A1300 has broader implications for astrophysics. The diffusion behavior of cosmic rays influences their energy distribution and the mechanisms of their acceleration and propagation through the universe, impacting the interpretation of high-energy astrophysical phenomena. The diffusion of particles contributes to the thermal and non-thermal dynamics in galaxy clusters, affecting the overall energy balance and the heating of the ICM. The results can inform models of magnetic field configurations in these clusters. Areas of low diffusion could indicate regions where magnetic field lines are particularly tangled or strong. The analysis of the diffusion coefficient in clusters A1656 and A1300 highlights the complex interplay between particle dynamics, energy loss mechanisms, and magnetic field structures. Understanding these relationships is crucial for interpreting high-energy astrophysical phenomena and advancing our knowledge of cosmic ray behavior in the universe. This analysis underscores the importance of further observational and theoretical studies to refine our models and improve our understanding of particle diffusion in astrophys-ical contexts. More study would be important on larger complete samples at high redshift to improve our understanding of non-thermal cluster properties and their correlation with cluster evolution. The present sample adds information on the low-power and small halos in bright and distant clusters, are in agreement with the size distribution as in the above figures 4.1, 4.2 and 4.3. Recently, the number

of new halos that are observed in clusters have been increasing. Therefore, the above information reported with the help X-ray indicated that the clusters should be continued in the future which opens the possibility that would report more significant detected diffuse radio emission sources in clusters.

CHAPTER 5

Summary and conclusion

5.1 Summary

Diffuse radio emission in galaxy clusters has become an increasingly important area of study in astrophysics. These emissions, known as diffuse radio emissions, are not directly tied to individual galaxies within the clusters but provide critical insights into the ICM, cosmic rays, and magnetic fields. Understanding these emissions is essential for unraveling the complex dynamics of galaxy clusters and their evolution over cosmic time. In galaxy clusters, three main types of diffuse radio sources are typically identified, each associated with different physical proces-ses. These are large, extended regions of radio emission found in the central areas of galaxy clusters. They are thought to be associated with ongoing merger processes and are indicative of turbulent ICM conditions. Found at the peripheries of clusters, radio relics are remnants of past merger events. They are often linked to shock waves that propagate through the ICM, accelerating particles and producing radio emissions. Smaller structures associated with cooling flows in clusters. Mini-halos are typically found around the central galaxies and are believed to be influenced by the activity of the central AGN. The primary electron model provides a framework for understanding the origins of the diffuse radio emissions observed in galaxy clusters. Primary relativistic electrons responsible for radio emissions can originate from several sources: High-energy processes associated with supermassive black holes can accelerate electrons to relativistic speeds. Supernova explosions and galactic winds can also contribute to the population of relativistic electrons

in the ICM. The model emphasizes the importance of re-acceleration mechanisms to sustain the energy of electrons in the ICM. As electrons lose energy through synchrotron radiation and inverse Compton scattering, turbulent motions, often triggered by cluster mergers, can re-accelerate these particles. The presence of shocks and turbulence in the ICM plays a crucial role in redistributing energy and maintaining the population of relativistic electrons necessary for the observed radio emissions. Recent observational campaigns, particularly those focusing on low-frequency radio emissions, have provided substantial evidence supporting the primary electron model. These observations have highlighted the significant contribution of AGN to the population of relativistic electrons in galaxy clusters. The correlation between AGN activity and increased radio luminosity in clusters suggests a direct link between these processes. The growing data base of observed diffuse radio sources allows for statistical analyses that reinforce the relationship between radio emissions, cluster dynamics, and the properties of the ICM. Studies of the spectral indices of radio halos indicate a consistent pattern that aligns with the predictions of the primary electron model, further validating the role of re-acceleration in maintaining the observed emissions. Understanding diffuse radio emissions through the lens of the primary electron model has broader implications for cosmology. In our analysis of the selected data on redshift (z) and power ($\log P(1.4)$) from the table. The table presents redshift values ranging from 0.023 to 0.307, alongside corresponding power values measured in logarithmic units ($\log P(1.4)$). The observed redshifts span from $z = 0.023$ (representing a nearby cluster) to $z = 0.307$ (indicating a more distant cluster). This range allows for the examination of how the properties of radio halos evolve as we look back in time. The power values ($\log P(1.4)$) are predominantly around 24, with a few instances of 23 and 25. The consistency in power values suggests that the radio emissions from the halos do not vary dramatically across this redshift range, at least within the observed clusters. The majority of the clusters exhibit a stable power output, indicating that the mechanisms driving radio emissions may remain relatively constant over this

range of redshifts. The slight deviations (from 23 to 25) could suggest subtle differences in halo properties, such as their magnetic field strength or electron density, which could influence the synchrotron radiation emitted. The observed stability in power across varying redshifts may imply that the physical processes involved in halo formation and maintenance are robust over time. This could indicate that clusters formed early in the universe continue to produce similar radio emissions as they evolve, which may be crucial for understanding the lifecycle of such structures. The X-axis represents redshift (z), measuring how much the wavelength of light has been stretched due to the universe's expansion. Higher redshift values indicate more distant and potentially older objects. The Y-axis represents luminosity distance, which measures how far away an object appears based on its brightness and the effects of distance in an expanding universe. The graph typically shows an increasing trend, where luminosity distance increases with redshift, reflecting that more distant objects appear dimmer. This relationship is fundamental in cosmology, helping to understand the scale and evolution of the universe. By examining the luminosity distance at various redshifts, researchers can infer how galaxy clusters' properties, such as mass and luminosity, evolve over cosmic time. The relationship illustrated in the figure supports the idea that the energy dynamics of radio halos may remain stable over time, suggesting that the mechanisms responsible for radio emissions in clusters do not change dramatically as the universe evolves. The X-ray luminosity in a merger is a strong indicator of the occurrence of major mergers between high mass systems. The redshift range is much narrower than the group sample, with most clusters lying at $z < 0.1$ and only a few reaching $z \approx 0.3$. High X-ray luminosity typically correlates with increased energy and temperature in the ICM, which can result from the dynamical activity of merging clusters. The observed redshift values primarily cluster around $z < 0.1$, indicating that most analyzed clusters are relatively nearby. A small number of clusters extend to $z \approx 0.3$, suggesting that while significant mergers are ongoing, they are predominantly observed in more recent cosmic times. The surface brightness values for the two clusters indicate a significant difference in the intensity of diffuse

radio emissions. A1656, with a surface brightness of 530 mJy, exhibits a strong radio halo, suggesting a dense population of relativistic electrons and/or a stronger magnetic field within the cluster. In contrast, A1300's surface brightness of 20 mJy suggests a much weaker radio halo, indicating a lower density of relativistic electrons or a less intense magnetic field. The higher surface brightness in A1656 may be attributed to ongoing astrophysical processes, such as active star formation and cluster mergers. The presence of young, energetic stars can accelerate electrons, contributing to synchrotron radiation. Interactions between galaxies in the cluster can generate shocks, further energizing particles and enhancing radio emission. The calculations for synchrotron and inverse Comp-ton scattering losses provide insight into how energy is dissipated in the clusters. The calculated synchrotron radiation loss of 3.39×10^{-27} W for both clusters indicates the efficiency of the magnetic field in converting kinetic energy of electrons into radiation. The inverse Compton scattering losses of 3.55×10^{-28} W suggest that the background photon field contributes to the energy loss of the relativistic electrons, particularly in environments with significant radiation fields. The cooling time for both clusters is approximately 1.36×10^{9} years. The relatively long cooling time suggests that the relativistic electrons can remain in the halo for extended periods before losing significant energy, indicative of a stable environment where electrons can accumulate and persist as a population. Understanding the diffusion coefficient in clusters like A1656 and A1300 has broader implications for astrophys-ics. The diffusion behavior of cosmic rays influences their energy distribution and the mechanisms of their acceleration and propagation. The diffusion of particles contributes to the thermal and non-thermal dynamics in galaxy clusters, affecting the overall energy balance. The results can inform models of magnetic field configur-ations in these clusters. The analysis of the diffusion coefficient in clusters A1656 and A1300 highlights the interplay between particle dynamics, energy loss mechani-sms, and magnetic field structures. Understanding these relationships is crucial for interpreting high-energy astrophysical phenomena.

5.2 Conclusion

The study of diffuse radio emission in galaxy clusters, particularly through the primary electron model, is a vital area of research that enhances our understanding of the complex interactions within the ICM. As observational techniques continue to improve, the insights gained from these studies will contribute significantly to our knowledge of cosmic structure formation, the behavior of cosmic rays, and the evolution of galaxy clusters over cosmic time. The observed halo radio power is likely influenced by ongoing major mergers within the clusters and the evolutionary history of the cluster over longer timescales. Recently, highlights strong evidence for the evolution of mergers with redshift, indicating that the merger fraction begins to increase around $z = 0.4$ undergo significant evolution from $z = 0.6$ to the present. The analysis enhances our understanding of individual galaxy clusters and contributes to the broader field of astrophysics by elucidating the connections between particle physics, electromagnetic processes, and cosmic structure formation. The stability of radio emissions across redshifts, the variations in surface brightness and X-ray luminosity suggesting ongoing major mergers influe-nce radio halo prope-rties, and the long cooling times and diffusion coefficients providing insights into the behavior and persistence of relativistic electrons in the clusters. Further studies on larger samples at high redshift are essential to improve our understanding of non-thermal cluster properties and their correlation with cluster evolution. The study of diffuse radio emissions provides insights into the evolutionary history of galaxy clusters. By examining the relationship between radio emissions and merger activity, researchers can infer the processes that govern cluster formation and evolution. Investigating the nature of diffuse radio emissions helps to elucidate the behavior of cosmic rays within the ICM and the role of magnetic fields in shaping the dynamics of clusters. Ongoing studies are crucial for exploring the mechanisms of particle acceleration and energy loss in greater detail. Future observations at higher frequencies and with improved sensitivity will likely reveal new aspects of the interplay between AGN activity, cosmic rays, and the ICM.

Bibliography

[1] RJ Van Weeren, F de Gasperin, H Akamatsu, Marcus Brüggen, L Feretti, H Kang, A Stroe, and F Zandanel. Diffuse radio emission from galaxy clusters. *Space Science Reviews*, 215(1):1–75, 2019.

[2] Surajit Paul, Ruta Kale, Abhirup Datta, Aritra Basu, Sharanya Sur, Viral Parekh, Prateek Gupta, Swarna Chatterjee, Sameer Salunkhe, Asif Iqbal, et al. Exploring diffuse radio emission in galaxy clusters and groups with ugmrt and ska. *Journal of Astrophysics and Astronomy*, 44(1):38, 2023.

[3] John R Helliwell. The evolution of synchrotron radiation and the growth of its importance in crystallography. *Crystallography reviews*, 18(1):33–93, 2012.

[4] G Giovannini, M Cau, A Bonafede, H Ebeling, L Feretti, M Girardi, M Gitti, F Govoni, A Ignesti, M Murgia, et al. Diffuse radio sources in a statistically complete sample of high-redshift galaxy clusters. *Astronomy & Astrophysics*, 640:A108, 2020.

[5] H-P Schlenvoigt, K Haupt, A Debus, F Budde, Oliver Jäckel, S Pfotenhauer, H Schwoerer, E Rohwer, JG Gallacher, E Brunetti, et al. A compact synchrotron radiation source driven by a laser-plasma wakefield accelerator. *Nature Physics*, 4(2):130–133, 2008.

[6] R Cassano and G Brunetti. Cluster mergers and non-thermal phenomena: a statistical magneto-turbulent model. *Monthly Notices of the Royal Astronomical Society*, 357(4):1313–1329, 2005.

[7] R Cassano, G Brunetti, and G Setti. Statistics of giant radio haloes from electron reacceleration models. *Monthly Notices of the Royal Astronomical Society*, 369(4):1577–1595, 2006.

[8] Luigina Feretti, Gabriele Giovannini, Federica Govoni, and Matteo Murgia. Clusters of galaxies: observational properties of the diffuse radio emission. *The Astronomy and Astrophysics Review*, 20(1):1–60, 2012.

[9] Helmut Wiedemann. Synchrotron radiation. In *Particle Accelerator Physics*, pages 647–686. Springer, 2003.

[10] Edward A Baltz and L Wai. Diffuse inverse compton and synchrotron emission from dark matter annihilations in galactic satellites. *Physical Review D*, 70(2):023512, 2004.